Chapter Six – Preliminary screen and condition optimisation for the miR-eGFP system

1. Introduction

As has been described in the previous chapter, an artificial miR-eGFP knockin cell line has been established, which contains a single copy of the mutagenic PB transposon knocked into the *Hprt* locus in *Blm*-deficient ES cells. ES cells with the miR-eGFP knockin express only 10 % of the eGFP level of cells without the miR-eGFP. ES cells with the miR-eGFP are sensitive to high concentrations (80 μg/ml or above) blasticidin (Chapter 5, Section 5.2.1.5.). Thus the phenotypic screening can be conducted using either FACs sorting based on eGFP expression levels or by direct select from the mutant pools using high concentrations of blasticidin.

FACs sorting would be an ideal screening method, as not only is it a direct phenotypic readout of the mutants, but it is also able to distinguish different classes of mutants based on the levels eGFP de-repression. Sorted cells can be plated in low density and the single cell-derived colonies can be picked and further analysed individually. However, this system may not work very efficiently when coupled with a recessive genetic screen based on the *Blm*-deficient ES cell system, as the frequency of pathway-relevant homozygous mutants is too low for cell sorting, Figure 6-1. Assuming that within 1,000 heterozygous mutants generated by PB transposon-mediated mutagenesis, one mutant is relevant to the miRNA biogenesis pathway. The rate of LOH in *Blm*-deficient ES cells is estimated to be 4.2×10^{-4} per cell per generation at a specific locus. Based on conservative estimates, the mutant pool needs to be expanded to 2.4×10^{6} cells to obtain a single homozygous mutant cell from one of the original heterozygous mutants. This means that the percentage of relevant mutants within the pool is 4.2×10^{-7}. This proportion of eGFP positive mutants is too low to be sorted successfully. However, if the mutants are enriched in a preliminary round of selection, a subsequent round of sorting may aid mutant isolation from the background. Therefore, using blasticidin selection as the primary screening scheme is a good choice.

Figure 6-1: Estimate of the proportion of homozygous mutants in the miRNA pathway.

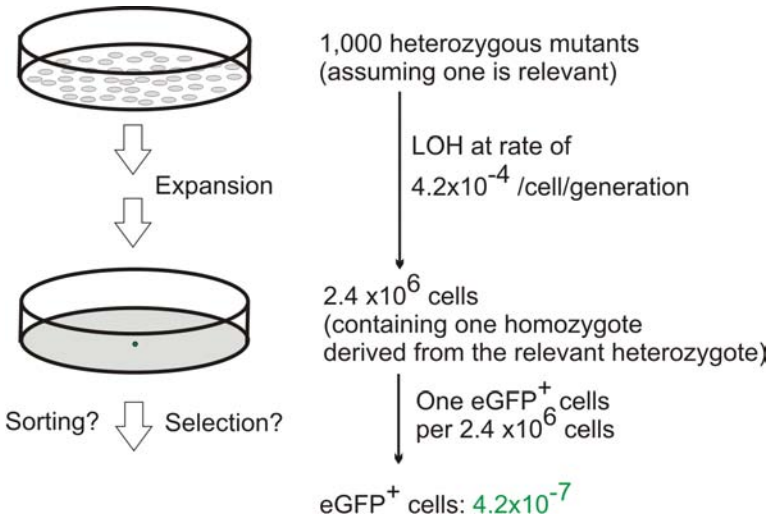

A detailed explanation is described in the main text.

In this chapter, different screening protocols have been tested for the isolation of homozygous mutants that are deficient in processing the miR-eGFP reporter. A known gene connected to the miRNA pathway, *Ago2*, has been identified during the preliminary screen and the validation of this mutant was also described.

2. Results

2.1. Generation of the mutant library

Figure 6-2 shows a schematic representation of mutant library generation. BlmHprtPBIn2miR-eGFP cells ($1x10^7$) were electroporated with 25 µg of a CMV-HyPBase expression plasmid and were divided and plated equally on three 90 mm plates. After three days of growth in M15, the cells from each 90 mm plate were trypsinised and an eighth of the cells were plated onto a fresh 90 mm plate. The next day, HAT and puromycin containing M15 was added to the plates and the selection continued for eight days until visible colonies formed. With this condition, around 600 to 800 colonies can be formed per 90 mm plate. The replating step conducted after electroporation with PBase was designed to allow transposition to proceed to completion before initiating selection. This disperses cells with different genotypes within a colony, so that the complexity of the mutant pool can be correctly estimated.

In total, ten electroporations were conducted and 30x 90 mm plates were selected to give rise to a total of 20,000 HAT and Puro double-resistant colonies. After HAT and puromycin selection, the colonies were recovered in M15 with HT supplemented for two days before the colonies were counted, trypinised to form single cell suspension and placed onto new 90 mm plates (one plate to one passage). When the 90 mm plates were confluent (containing about $2x10^7$ cells/90 mm plate), the culture should contain at least a few homozygous mutants per locus. In this procedure, the mutant library was sectored into 30 sub-libraries which were propagated independently, this mutants arose from different sub-libraries should be derived from independent heterozygous mutants. This should avoid the daughter cells of a dominant clone to populate the entire library, making the identification of other mutants difficult. Therefore in a typical screen, a few sub-libraries should contain colonies which are derived from the same homozygous mutant, while most of the sub-libraries do not contain any mutants.

Figure 6-2: Schematic representation of the mutant library construction.

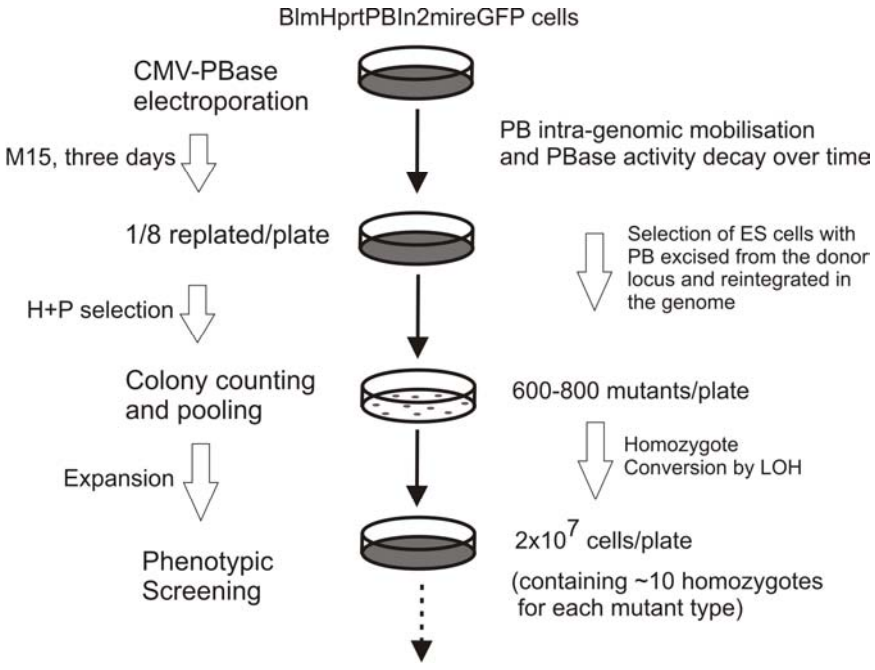

The flow chart to the left of the diagram describes the experimental procedures used for library generation; the flow chart to the right of the diagram describes the events occurring in the cell culture for each step during the library construction.

2.2. Screening strategies and optimisation

Four protocols were investigated for the phenotypic screening strategy, Figure 6-3.

Figure 6-3: Screening strategies for the miR-eGFP system.

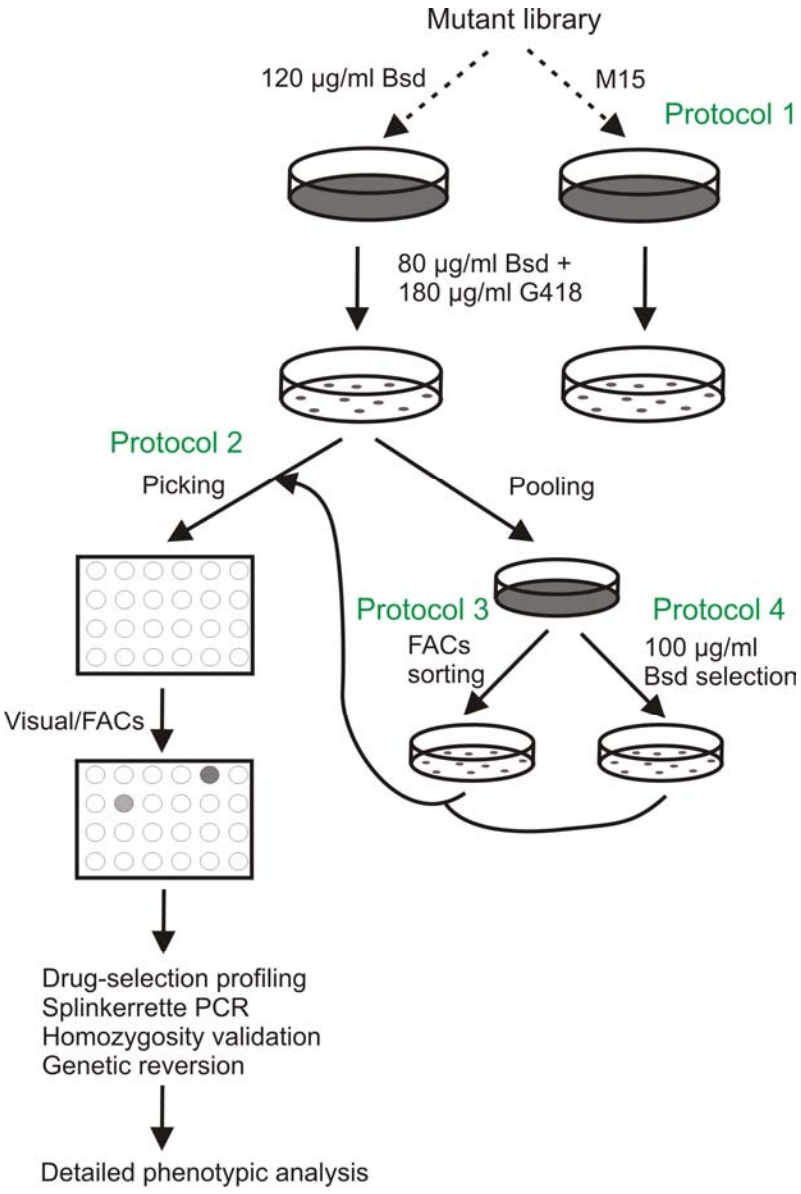

In total four protocols were tested and a detailed description is given in the main text below.

The first protocol (Protocol 1) was conducted by directly passaging the mutant cells from the library to 150 mm culture plates with a monolayer of blasticidin and G418 resistant feeders. The next day, 80 μg/ml blasticidin and 180 μg/ml G418 containing M15 was applied to the cells and the selection was maintained for eight days. Many cells survived the selection and each plate was covered with approximately a thousand colonies at the end of the selection and there was no difference observed among the plates. This might have been caused by the high cell density and the inefficiency of Bsd-mediated killing of cells with residual 10% eGFP-IRES-Bsd expression. Therefore, protocol 1 was not sufficient for the relevant mutant selection.

In order to enhance the selection sensitivity, the cells from the established mutant library were passaged onto 150 mm plates with M15 containing 120 μg/ml blasticidin. This concentration of blasticidin was tested during the cell line validation analysis (Chapter 5 Section 5.2.1.5.). Under this selection, the cells without the miR-eGFP can survive albeit a slight reduced growth rate for up to six days. The next day, 80 μg/ml blasticidin and 180 μg/ml G418 dual-selection was initiated and maintained for eight days. Under these conditions, there were approximately 50 ~ 300 colonies formed on each plate with some plates containing significantly more colonies than others, indicating that there may be mutants present. The majority of the plates with low number of colonies may reflect the background of this selection scheme.

Three protocols were used after this initial blasticidin selection. In Protocol 2, twelve individual colonies were directly picked from each mutant pool and in total 360 colonies were picked from the whole library and examined for eGFP intensity either manually under the fluorescent microscope or by high-throughput FACs analysis using 96 well plates. In Protocol 3 and 4, the colonies generated from the initial blasticidin selection were first pooled with three other pools to form ten super-pools. These ten pools were passaged twice and were either FACs sorted (Protocol 3), or plated onto 90 mm culture plates for a second round of blasticidin selection with slightly elevated blasticidin concentration, 100 μg/ml. The colonies

which resulted from these protocols were picked and subjected to eGFP intensity analysis as described previously.

In total, 13 eGFP-positive colonies were isolated from all three protocols, they were subjected to drug-selection profiling using HAT, puromycin and G418 to confirm their phenotype. The Splinkerette PCR was then conducted on the clones with the correct drug-selection profiles to identify the PB transposon insertion sites. Upon locus identification, the homozygosity status of the locus and further detailed phenotypic analysis could proceed.

The results of Protocol 2, 3 and 4 are shown in Table 6-1. Using protocol 2, only one out of the 360 colonies picked showed eGFP expression. By FACs analysis, the eGFP expression level in this mutant was equal to the eGFP level in the cells without miR-eGFP reporter. Splinkerette PCR indentified the PB transposon was inserted into *Ago2*, which is known for its involvement in miRNA/siRNA-mediated gene silencing. The detailed validation of this mutant is described in the next section of this chapter.

When protocols 3 and 4 were used, 12 eGFP positive colonies were identified and confirmed by FACs analysis. These colonies were derived from three main pools, thus they may be daughter clones originating from single mutant genotypes. The *Ago2* mutant was identified from pool No. 5 using Protocol 2, the eGFP positive clones obtained from pool No.13/14/15 were not *Ago2* mutants. In total from both protocols, three clones were derived from pool No.1/2/3, four clones from pool No. 13/14/15 and five clones from pool No.7/8/9 and one clone from pool No. 25/26/27.

These 12 clones were examined for their resistant or sensitivity to puromycin, G418, and HAT to further confirm their genotypes. Puromycin resistance confirms the presence of the PB transposon within the ES cell genome and all the clones analysed were puromycin resistant. The sensitivity to G418 suggests the loss or silencing of the miR-eGFP, which can give rise to elevated eGFP expression, thus, clones with this phenotype will not be true mutants. Four

clones were identified as being G418 sensitive (two clones from pool No.1/2/3 and one clone from pool No. 25/26/27), Table 6-2.

HAT resistance confirms the excision of PB transposon excision from the donor site. However, spontaneous mutation in the *Hprt* locus after PB excision from the locus can also give rise to a HAT sensitive phenotype. The nine clones from two pools (four from pool No. 13/14/15, and five from No. 7/8/9) were HAT sensitive. The Splinkerette PCR was performed on 36 clones including all the eGFP-positive clones and randomly selected eGFP-negative background clones. For 33 clones including all eGFP-positive clones, the PCR products were mapped at the donor *Hprt* locus. The four clones consisted of two independent PB integration sites with two eGFP-negative sister clones (Clone 22 and 23) and two eGFP-positive sister clones (Clone 2 and 3). The PB integration in Clone 2 and 3 was mapped to X chromosome 3' of the *Hprt* coding region with coordinate 50,380,002 337 (NCBI Build37), Table 6-2, while the PB integration in Clone 22 and 23 was mapped to a intergenic region on *X* chromosome with coordinate 116,735,337 (NCBI Build37).

Southern blotting was conducted on all these clones to detect the pattern of PB integrations. A PB5'TIR probe was used to detect PB intra-genomic mobilisation, Figure 6-4. The southern blotting results confirmed the Splinkerette PCR result, with most of the clones showing a band pattern identical to the control sample, the cell line before PB mobilisation. The only four clones with different band patterns matched the four eGFP-negative clones with PB away from the *Hprt* donor site, identified from the Splinkerette PCR. This data suggests that there were a significant proportion of cells present in the mutant pools without the mobilisation. Their survival under HAT selection during the library construction was most likely due to the known strong cross-rescue effect among cells close by. Therefore, the clones that were HAT sensitive but their eGFP-positive expression may be due to spontaneous mutations within the miRNA processing pathways.

Table 6-1: Efficiency comparison between screening protocols.

	Protocol 2	Protocol 3	Protocol 4
No. colonies	~ 6,000	~ 400	~ 60
No. picked	360	170	50
No. eGFP+	1	7	5

Table 6-2: Summary of the identities of eGFP-positive clones.

	Protocol 2	Protocol 3	Protocol 4
Total no. eGFP+	1	7	5
Clonal relation*	Pool No.13	A, 2 from pool No.1/2/3 B, 4 from pool No.13/14/15 C, 1 from pool No.25/26/27	B, 5 from pool No.7/8/9
Drug-profile	HAT^R, $Puro^R$, $G418^R$	Type A: HAT^R, $Puro^R$, $G418^S$ Clone 2 and 3 Type B: HAT^S, $Puro^R$, $G418^R$ Clone 4,5,6 and 7 Type C: HAT^R, $Puro^R$, $G418^S$ Clone 1	Type A, HAT^R, $Puro^R$, $G418^S$ Clone 8 Type B, HAT^S, $Puro^R$, $G418^R$ Clone 9, 10, 11, and 12
Splinkerette PCR (Candidate locus)	*Ago2*	Type A: *X* chr.: 50,380,002 Others were mapped to the donor site#.	All were mapped to the donor site.
Comments	Intron 1 of *Ago2*	Type A, *X* chr.: 50,380,002 3' downstream *Hprt*#.	N/A

*: clonal relation between different clones isolated from the same pool was classified based on the G418, puromycin (Puro) and HAT resistant phenotype A, B, and C. The clone I.D. was followed by the drug-resistant phenotype and is consistent with the clones shown in the Southern blot in Figure 6-4b. #: the two sister eGFP-positive clones (Clone 2 and 3) were mapped to a genomic location 3' to the *Hprt* coding region and the genomic coordinate is based on NCBI Build37.

Figure 6-4: Southern detection for the PB transposon reintegration patterns.

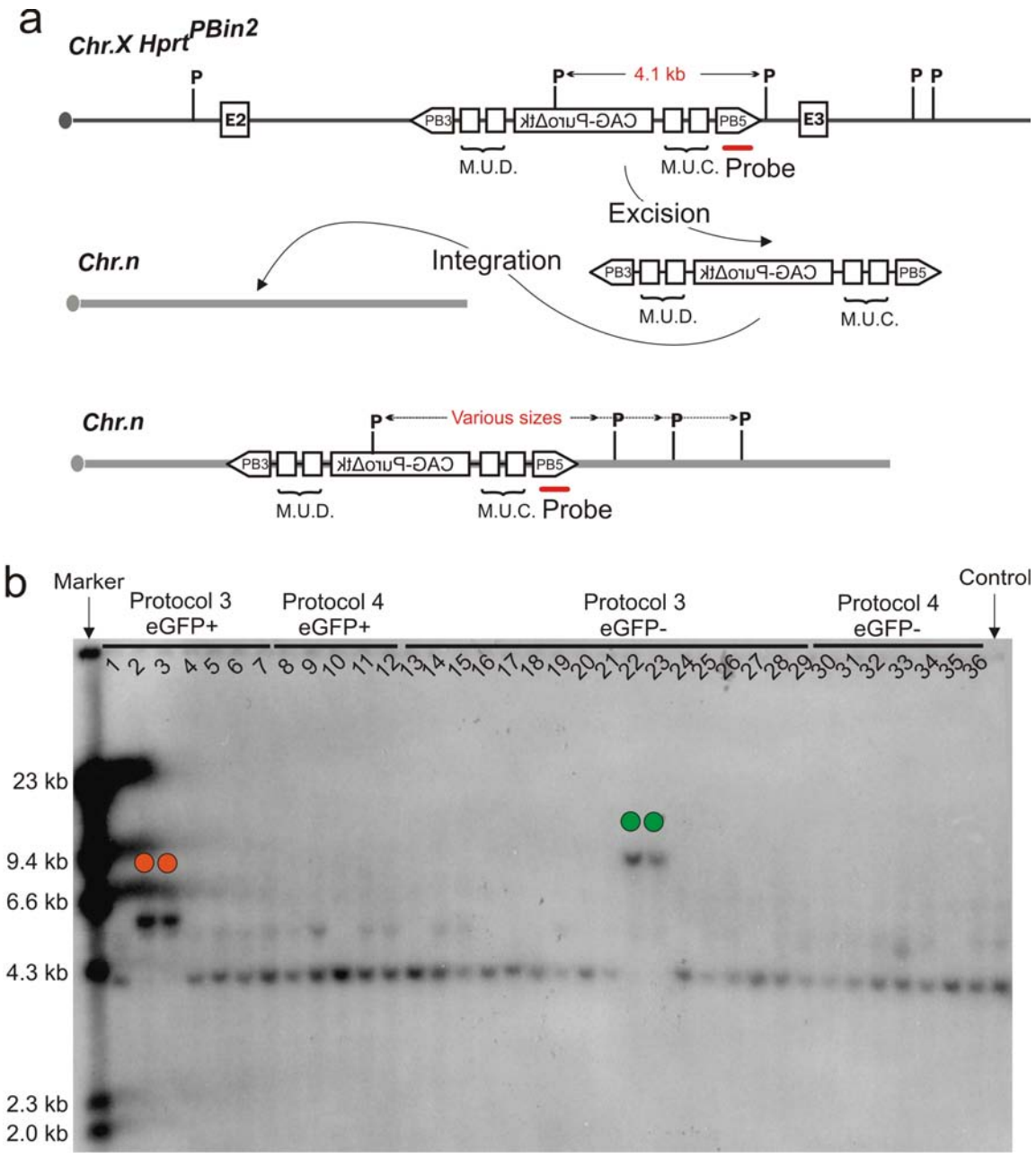

a, Southern detection scheme for the PB integration sites. When the PB transposon was located in the *Hprt* locus, the Southern blot gave rise to a band with 4.1 kb in size when the genomic DNA was digested with *Pst*I. When the PB transposon re-integrated elsewhere in the genome, the band pattern will alter depending on the sequences of the specific integration sites. P, *Pst*I site. b, Southern blotting results of all eGFP positive clones identified from Protocol 3 and 4 and some random clones picked from the pool. Control, DNA extracted from ES cells without PB mobilisation. Only the clones with red (two sister clones from pool No.1/2/3) or green (two sister clones from pool No.19/20/21, randomly selected) dots indicated showed PB reintegration events, and the two red marked clones were derived from the same pool, and the green clones from another pool.

2.3. Mutant validation

The *Ago2* mutant identified from Protocol 2 was further analysed, Figure 6-5. The mutagenic PB transposon was inserted in intron 1 of the *Ago2* gene. The *Ago2* inactivation was mediated by the Ccdc107 mutagen unit, based on the orientation of the PB integration and confirmed by the fusion RT-PCR product detected in the mutant clone, Figure 6-5a,c. Genomic PCRs were conducted with primers specific to the locus and PB-specific primers to validate the homozygosity status of this mutant, Figure 6-5b. In the mutant, the wild-type PCR product generated by two locus specific primers spanning the PB integration site was completely absent; whereas PCR products were produced when the PB transposon-specific primers and the locus-specific primers near the integration site were used. The opposite was observed in wild-type cells. Therefore, the mutant must be homozygous with both alleles inactivated by the mutagenic PB transposons. RT-PCR analysis on the mutant confirmed a null mutant phenotype, as no wild-type transcript was detected, when both 5' and 3' end of the transcripts were analysed. The fusion transcript detected in the mutant showed the correct fragment size as predicted. The doublet band-pattern indicates the alternative splicing in the intron of the Ccdc107 mutagen between the two exons as observed previously (Chapter 3). Finally, the eGFP expression profile showed that the mutant had an elevated eGFP level equivalent to the reporter cell line without the miR-eGFP, Figure 6-5d. Taken together, the Ago2 mutant clone found is truly a homozygous null mutant with the defective miR-eGFP-mediated eGFP silencing.

Figure 6-5: *Ago2* mutant molecular analysis.

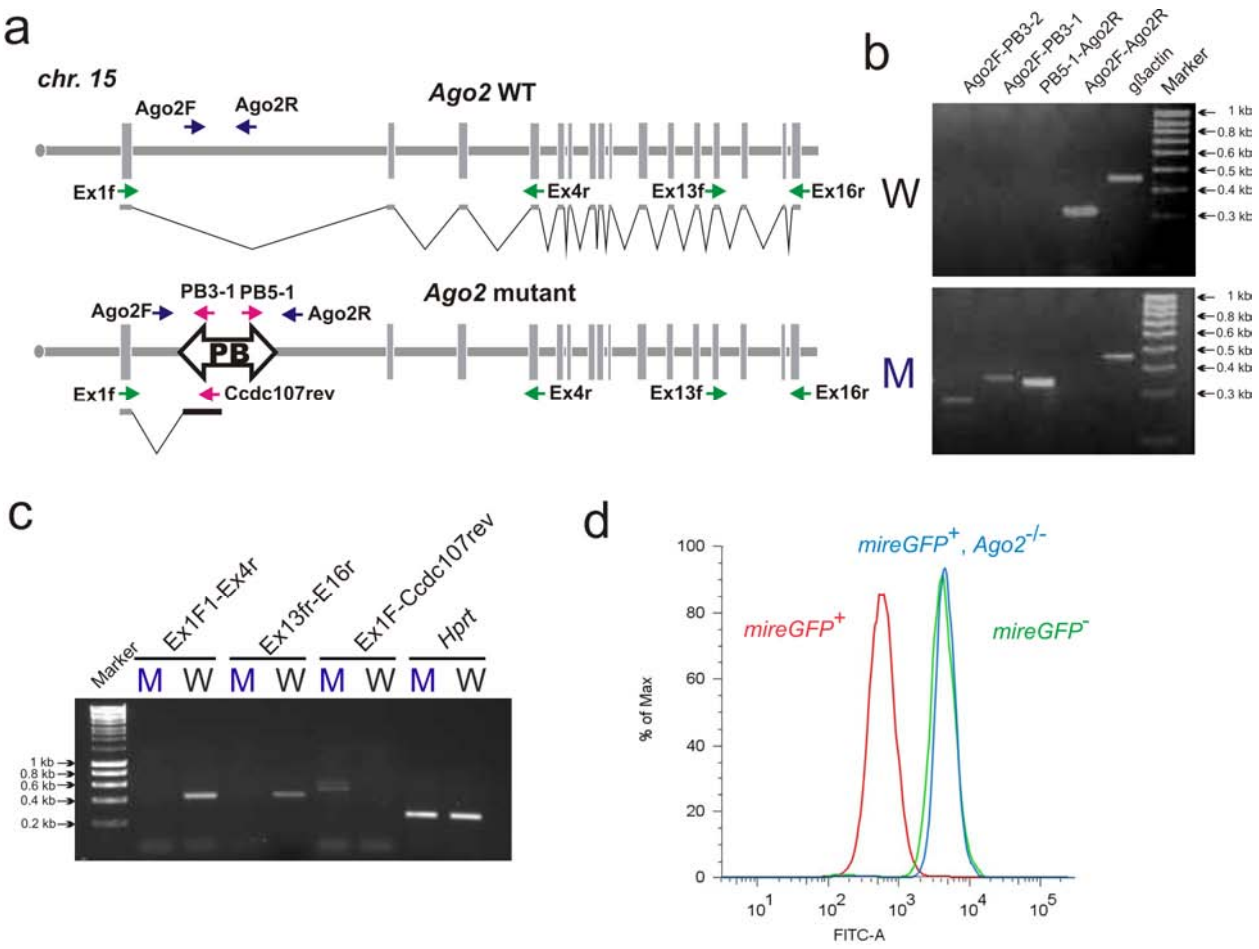

a, PB integration site within the *Ago2* locus and the predicted trap-based gene inactivation. b, genomic-PCR validates the homozygosity status of this clone. W, wild type control, M, *Ago2* mutant. The absence of the wild-type PCR product suggests that *Ago2* mutant is homozygous. c, RT-PCR analysis of the *Ago2* transcript in mutant and wild-type cells. d, FACs profile on the eGFP expression of the *Ago2* mutant. The positive control was ES cells without miR-eGFP targeted and the negative control is the cells with miR-eGFP targeted but without PB mobilised.

3. Discussion

3.1. Future improvement on the miR-eGFP screening system

This chapter describes a preliminary screen using the miR-eGFP system and various experimental strategies to optimise the screening procedure. A homozygous mutant *Ago2*, a key component in the miRNA/siRNA-mediated silencing was identified from this initial attempt. The ability to identify a known gene in the pathway confirmed the success of the design and performance of the recessive-screening strategy. Further experiments can be conducted using the established protocols to identify novel components in the pathway. However, during this preliminary study, two existing problems have also been identified. These outstanding problems could be a reason why only one hit was found. These problems will be addressed before subsequent rounds of screening are conducted to increase the capacity of novel mutant identification.

Firstly, the mutant library contained a limited representation of heterozygous mutants which was not correlated with the estimated complexity. The main cause was likely to be the post-electroporation replating and selection scheme which favoured the survival of cells without PB transposon excised from the donor locus. Although such cells should be sensitive to HAT, they can survive by sharing the metabolites generated by surrounding *Hprt* proficient cells in the mixed population that had PB excised from the *Hprt* locus. One way to avoid this would be to initiate HAT selection directly after the PBase-electroporation without the replating to avoid such an issue.

Secondly, PB excision from the donor site did not seem to be very efficient, judging by the total colony number obtained after selection compared to previous data obtained using the identical locus and transposon. In addition, the two integration sites mapped in clones isolated after blasticidin selection were both having PB transposons integrated on *X* chromosome near the donor site. Thus, in this preliminary screen, genome-wide mutagenesis was not achieved to a satisfactory level. The reason for inefficient PB intra-chromosomal mobilisation of PB was not clear, although *Blm* deficiency may negatively affect the repair of the double-strand breaks of the genomic DNA after PB excision. Local-hopping of the PB

transposon means that more HAT and puromycin resistant mutants need to be generated in order to achieve genome-wide coverage compared to mutagenic strategies with no local-hopping effect. Therefore with the current system, the degree of local hopping should be estimated in order to generate a large enough library to provide a good coverage of the genome. Alternatively, the plasmid-to-genome mobilisation method may be reconsidered for generating the library.

Apart from the limitation posed by the mutagenesis coverage, the mixed-mutant pooling strategy used for the *Blm*-deficient ES cell system has an intrinsic limitation in isolating mutants that have growth defects. The LOH rate estimation was based on the assumption that homozygous mutants of interest possess the same growth rate as other cells present in the pool. However, mutants with reduced growth rates will expand slower than other cells in the pool, thus the number of homozygous mutant cells from such clones within the pool would be less than expected. Overtime, the proportion of this type of homozygous mutant will drop significantly as they are out-competed by others. Both miRNA-biogenesis mutants *Dgcr8* and *Dicer* show retarded growth and due to the loss of ESCC miRNAs, described in Chapter One (Kanellopoulou et al., 2005; Wang et al., 2007). Therefore, in this screen, mutants like *Dgcr8* and *Dicer* may not be easily identified, but this should still be possible, since these cells are viable and can proliferate. If LOH of these mutants occurred early during expansion, they could still contribute a decent proportion within the pool. In further screens, enrichment strategies should be conducted as early as possible to reduce the risk of such mutants being out-competed. Cell-cycle rate compensation of the mutants may also be possible by introducing transgenic cell cycle effectors that are regulated by ESCC miRNAs or parallel to ESCC miRNA regulation. Thus, upon loss of miRNAs in the mutants, the cell-cycle defect might be rescued by the exogenous expression of the introduced gene to compensate the effect downstream of ESCC miRNA regulation. For example, genes such as *C-myc* may partly compensate the loss of ESCC miRNAs since *C-myc* has been shown to be able to transcriptionally repress the cell cycle inhibitor Cdk1na, which is a major target of ESCC miRNAs which reduces the G1-S cell-cycle transition (Seoane et al., 2002).

Screening protocols 2, 3 and 4 were able to identify eGFP-positive cells. Despite the low efficiency of obtaining eGFP-positive clones in Protocol 2, this is the only protocol which produced a genuine hit. The failure to identify the same hits in Protocols 3 and 4 may due to the fact the proportion of the mutant in the sub-pool may be very limited, and the further pooling of sub-pools would have reduced the proportion of this mutant and it may have been lost during passages before the pools were subjected to secondary enrichment. The ability to isolate eGFP-positive clones using protocols 3 and 4 suggest that these methods are capable of isolating potential mutants. The inability to detect sister clones from the same clonal origin may reflect the fact that there were no genuine mutants present in these pools and the false positive mutants identified may have arisen after the culture was split. The use of FACs sorting to enrich mutants in Protocol 3 may be potentially less "invasive" to cell growth than use of high concentration of blasticidin. Therefore, in the future screening, the combined use of protocols 2 and 3 could be sufficient for mutant isolation and enrichment, with minimal passages before the FACs sorting in protocol 3.

3.2. *Ago2*, Argonaute proteins and the small RNA mediated pathways

The homozygous mutant identified in this preliminary screen was *Ago2*, also known as *Eif2c2*. Ago2 is one of the mammalian Argonaute proteins playing key roles in small RNA-mediated regulatory pathways that modulate gene expression, chromosome structure and function, and provide a defense mechanism to silence invading viruses and transposons. A *Blm*-deficient ES cell based recessive screen for siRNA processing pathway also identified *Ago2* as a key player in siRNA-mediated gene silencing (Trombly et al., 2009). In that screen, multiple but independent hits within intron 1 of *Ago2* were identified, highlighting the high degree of bias for retrovirus integrations within certain regions of the mammalian genome.

The Ago family can be sub-divided into three clades, the Piwi clade, which are closely related to *D. melanogaster* PIWI (P-element induced wimpy testis), the Wago clade, which are specific to *C. elegans* and the Ago clade, which are similar to *Arabidopsis thaliana* AGO1 (Hutvagner and Simard, 2008). The piwi clade is not present in plant, and plays a role as part of the innate immune system to silence mobile genetic elements in the nucleus. The Ago-

clade members are found in both plant and animal species and are effectors in small RNA-mediated gene regulation.

The protein structures of Argonautes are well conserved, consisting of four distinct domains, the N-terminal, PAZ, Mid, and PIWI domains. The PAZ and Mid domains facilitate the anchoring of the small RNA guide, with PAZ binding the 3′ end using a series of conserved aromatic residues and the Mid domain providing a binding pocket for the 5′ end. In addition, the Mid domain of metazoan Argonautes that function in the miRNA pathway contain a motif known as the MC domain, which has homology to the cap structure binding motif of the translation initiation factor eIF4E, and it may function to interfere with translation (Kiriakidou et al., 2007). The PIWI domain contains an RNase-H-like fold, which evolved to use ssRNA as a template to target RNA with highly complementary sequence. Ago brings the scissile phosphate, opposite to the 10^{th} and 11^{th} nucleotides of the small RNA guide, into the enzyme active site of the PIWI domain to conduct the RNA cleavage, leaving 5′ P and 3′ OH termini. In mammals, Ago2 is the only Ago members out of four members Ago1-4, to maintain the endonuclease (slicer) activity. Other Ago-clade members have lost their cleavage activity during evolution.

A few miRNAs have been found to use cleavage-mediated gene repression in mammals (Yekta et al., 2004), thus Ago2 is important in mediating miRNA function. However, in mammals, the majority of the miRNA-mediated gene repression uses translational repression to regulate target gene expression. Although this mode of gene regulation does not require the slicer activity of the Ago protein, several mature miRNAs which use the translational repression-mediated effector pathway showed a significant decrease in their steady-state expression level in the absence of Ago2 (Diederichs and Haber, 2007; Kaneda et al., 2009). This suggests that Ago2 may also play an active role in miRNA biogenesis or stabilisation of mature miRNAs.

A novel miRNA intermediate (ac-pre-miRNA) structure of several miRNAs was discovered which was shown to be an Ago2 cleaved pre-miRNA hairpin, and it can be subsequently processed by Dicer complex (Diederichs and Haber, 2007). Whether this intermediate is a by-

product generated during Ago2-Dicer complex association or has biological significance is unclear. This novel Ago2 processing function may be independent from the RISC-mediated effector action, aiding Dicer cleavage to enhance miRNA biogenesis. This may explain the drop in the steady-state level of some miRNAs observed when Ago2 is absent. Processing with Ago2 may also be biologically significant. So far one miRNA, mir-451, has been found to rely purely on the Ago2-dependent processing to generate a structure similar to the ac-pre-miRNA and can bypass the Dicer step in its maturation (Cheloufi et al., 2010).

In plants and *C. elegans*, some Argonaute proteins that are involved in both exogenous and endogenous RNAi pathways can mediate secondary siRNA production, which is important in maintaining and propagating the RNAi response (Yigit *et al.*, 2006; Hutvagner and Simard, 2008). Once a *de novo* dsRNA duplex is generated, the siRNA can serve as the primer to generate new siRNAs (the secondary siRNAs) by RNA-dependent RNA polymerases (RdRPs). These products are then either cleaved by Dicer or other RNase-III-like enzymes and are subsequently loaded onto catalytic or non-catalytic Ago proteins to induce another level of gene silencing. In mammals, it is thought that such an endogenous RNAi response is not permissive due to the long-dsRNA induced interferon response, which leads to global translation termination, RNaseL induction and apoptosis. In addition, the mammalian homologue RdRP has not been found at this time.

Recently there have been two breakthroughs in proving the presence of endogenous RNAi in mammals. Firstly, mammalian endo-siRNAs have been identified in oocytes and ES cells (Babiarz et al., 2008; Tam et al., 2008; Watanabe et al., 2008), suggesting that the endogenous RNAi pathway is indeed present in mammals. The presence of endo-siRNAs in oocytes and ES cells is attributed to the lack of interferon responses in these cells. Oocytes with a knockout (both maternal and zygotic) of either *Dicer* or *Ago2* show severe defects in oocyte meiosis I and II and the global mRNA expression varied significantly from the wild-type situation (Murchison *et al.*, 2007; Kaneda *et al.*, 2009). Furthermore, knocking down Ago2 but not Ago3 or 4 in the two-cell stage mouse embryos can lead to developmental arrest (Lykke-Andersen et al., 2008). Finally, oocytes with a Dgcr8 knockout are phenotypically normal

without any global mRNA expression change (Suh et al., 2010). These data highlight the essential roles endo-siRNAs play in mammalian oogenesis and early zygotic development. Another seminal discovery is the identification of mammalian RdRP equivalent, formed by the telomerase reverse transcriptase catalytic subunit (TERT) and the RNA component of mitochondrial RNA processing endoribonuclease (RMRP) (Maida et al., 2009). Therefore, mammals do possess the endogenous siRNA pathways and the understanding of endo-siRNA biogenesis and its effector pathways as well as their functions in mammalian early development is a very exciting area of research.

In summary, being a unique Ago-clade member with endonuclease activity, Ago2 is involved in many areas of small RNA biogenesis and regulation. Figure 6-6 summarises the different roles of Ago2 in mammalian systems. Considered together, the use of small RNA biogenesis/effector pathway mutants has provided us with significant knowledge in understanding the roles these small non-coding RNAs play in many areas in biology. However, components in the biogenesis and effector pathways are still not fully uncovered. Novel mutants will further aid our understanding of the fundamental roles non-coding small RNAs play in biology.

Figure 6-6: Multiple roles of Ago2 in the non-coding small RNA biogenesis, regulation and effector pathways.